Structure, thermal stability, and optical properties of boron modified nanocrystalline anatase prepared by chemical vapor synthesis

Imteyaz Ahmad Md.,[1,a)] S. S. Bhattacharya,[1,b)] and Horst Hahn[2,c)]
[1]*Department of Metallurgical and Materials Engineering, Indian Institute of Technology Madras, Chennai 600036, India*
[2]*Joint Research Laboratory Nanomaterials, Technische Universität Darmstadt and Forschungszentrum Karlsruhe, 64287 Darmstadt, Germany*

(Received 23 January 2009; accepted 4 May 2009; published online 10 June 2009)

Boron modified nanocrystalline anatase titania powders with boron contents varying from 0.5 to 6.2 wt % were synthesized by a chemical vapor synthesis process. High temperature x-ray diffraction studies revealed that the anatase powders containing more boron were more stable at higher temperatures. When present in small quantities (about 0.5 wt % or less), boron went into the structure of titania and lowered the direct band gap to 3.41 eV. On the other hand, higher boron contents resulted in smaller anatase crystallite sizes and partially offset the redshift. However, the excess boron formed boron oxide which probably coated the surface of the nanoparticles/crystallites resulting in improved high temperature stability of the anatase phase. © *2009 American Institute of Physics*. [DOI: 10.1063/1.3143029]

I. INTRODUCTION

Anatase titania in the nanocrystalline form has recently received a lot of attention due to its applicability in photocatalysis, photovoltaics, antibacterial, and self-cleaning coatings.[1–4] The superior catalytic properties of nanocrystalline anatase arise from the higher specific surface area and greater number of reaction sites when compared to its microcrystalline counterpart. The band gap of microcystalline anatase is reported to be 3.19 eV due to an indirect transition from the center to edge of the Brillouin zone ($\Gamma_3 \rightarrow X_{1b}$) while the lowest allowable direct transitions at the edge of the Brillouin zone $X_{1a} \rightarrow X_{1b}$ and $X_{2b} \rightarrow X_{1b}$ result in band gaps of 3.41 and 3.59 eV respectively.[5–7] It has been well documented that the band gap of titania (both direct and indirect) increases when the crystallite sizes are decreased to nanocrystalline levels.[8] This results in the absorption edge being shifted further into the UV regime, thereby resulting in lower utilization of the sunlight spectrum during photocatalysis. At the same time, the higher driving force for grain growth and more number of potential sites for rutile nucleation[9–11] cause the anatase nanocrystallites to grow rapidly on heating and transform into the stable rutile phase. Although micron-sized anatase powders start transforming to rutile at about 700 °C, nanocrystalline anatase may start transforming at a temperature as low as 500 °C.[12,13] Therefore, synthesizing nanocrystalline anatase with lower band gap and high temperature stability is one of the key challenges.

In order to reduce the band gap of anatase, many studies have been dedicated to the doping of titania with metals as well as nonmetals. Doping with metals such as Ni, Fe, Cr, Co, etc., has the primary drawback of thermal instability and formation of intermediate phases.[14] By far, nonmetallic dopants such as N, B, S, C, etc., have shown encouraging results without contributing much to the stability of the anatase phase.[15–19] Baiju *et al.*[20] studied the effect of lanthanum doping which stabilized the anatase phase to temperatures above 800 °C. There have been several attempts to stabilize the anatase phase at higher temperatures by means of doping with metal oxides such as NiO, Al_2O_3, ZrO_2, and SiO_2.[21–23] Doping with these oxides stabilized the anatase phase to a temperature up to 1000 °C. Presence of other oxides at the grain boundaries, introduction of oxygen vacancies and lattice strain due to doping are some of the mechanisms proposed to rationalize the stabilization of anatase to higher temperatures.[24,25] Yang and Ferriera[26] studied the individual and combined effect of Al_2O_3 and SiO_2 on titania which stabilized anatase up to a temperature of 1100 °C. However, formation of secondary intermediate, but unwanted phases (Al_2TiO_5, $NiTiO_3$) are major drawbacks of this approach. Carbon doping in TiO_2 has been reported to increase stability of anatase at higher temperatures.[27] It has also been demonstrated that the temperature range of anatase to rutile transformation depends on the processing conditions during synthesis.[28,29]

Boron doping in titania has shown encouraging results in stabilizing the anatase phase to higher temperatures as well as exhibiting an improved photocatalytic response.[30,31] There have been, however, some contradictory reports on the effect of boron doping on the band gap of titania. Some reports showed a redshift due to boron[31] while the others suggest that boron causes a blueshift.[30] Yang *et al.*[32] showed theoretically from density functional calculations that the presence of boron at substitutional sites (O or Ti) resulted in a redshift whereas a blueshift resulted when boron was present at interstitial sites. There has also been evidence of boron oxide formation on heating the samples containing sufficient quantity of boron[30] indicating limited solubility of boron in tita-

[a)]Also at Joint Research Laboratory Nanomaterials, Technische Universität Darmstadt and Forschungszentrum Karlsruhe, 64287 Darmstadt, Germany.
[b)]Electronic mail: ssb@iitm.ac.in. FAX: +914422574752.
[c)]Also at Institute for Nanotechnology, Forschungszentrum Karlsruhe, 76021 Karlsruhe, Germany.

 © 2009 American Institute of Physics

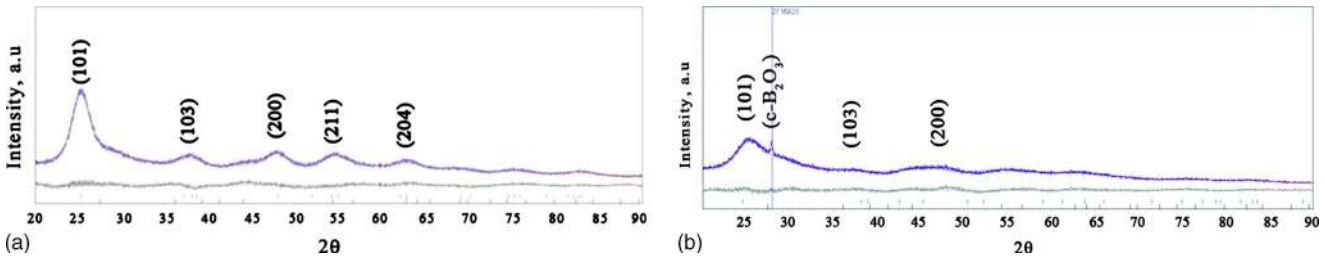

FIG. 1. (Color online) XRD patterns (Cu $K\alpha$) of the nanocrystalline titania samples having (a) 0.5 wt % boron and (b) 1.89 wt % boron. Presence of cubic B_2O_3 was revealed in the XRD pattern of the sample with higher boron content.

nia. There have been very few studies undertaken on the effect of boron addition to anatase covering the aspects of band gap change and anatase stability. In the present work, boron modified nanocrystalline titania in anatase form was synthesized by a chemical vapor synthesis process with varying boron content. The stability of the anatase phase and photoluminescence was studied.

II. EXPERIMENTAL

In a chemical vapor synthesis process, a metallorganic precursor is decomposed/pyrolized at a high temperature within the well defined reaction zone of a hotwall reactor and the nanocrystalline metal oxide powders that are produced as a result are deposited in a collector unit.[33–36] In the present study titanium tetraisopropoxide was fed into a hotwall reactor (tubular furnace) through a bubbler using helium as carrier gas at a flow rate of 500 SCCM (SCCM denotes cubic centimeter per minute at STP). Oxygen was supplied at a constant flow rate of 1000 SCCM and triethyl boron vapor was supplied through a separate bubbler at different flow rates of 2, 3, 5, 10, and 20 SCCM in order to vary the boron content in the resultant B-modified TiO_2 powders. The hotwall reactor was kept at a temperature of 800 °C and the system pressure maintained at 10 mbar through a closed-loop pressure control system involving a butterfly valve, a baratron pressure gauge, a proportional-integral-derivative controller, and a vacuum pump. The synthesized powders were deposited in a thermophoretic collector made of a meandered, water-cooled chamber with quartz lamps.

The composition of the synthesized powders was estimated by atomic emission spectroscopy using inductively coupled plasma in a Perkin Elmer Optima 3000 machine. The specific surface areas and degree of agglomeration was estimated by nitrogen adsorption using the multipoint Brunauer-Emmett-Teller (BET) approach in a Quantachrome Autosorb automated gas sorption system. Additionally, the amount of boron and its oxidation state were ascertained by x-ray photoelectron emission spectroscopy (XPS). The powders were also characterized by solid state NMR using a Bruker Advanced® 400 NMR spectrometer and a Perkin Elmer 1750 infrared Fourier transform spectrometer was used to record the Fourier transform infrared spectroscopy (FTIR) spectrum.

Room temperature x-ray diffraction (XRD) patterns were recorded in a Siemens D5000 machine, for all the samples in the 2θ range of 20°–90° with a step size of 0.02° and exposure time of 12 s using Cu $K\alpha$ radiation. The high temperature phase stability was studied in a high temperature Bruker D8 x-ray diffractometer. XRD patterns between the 2θ values of 20° and 35° were recorded at 300, 500, 700, 800, 900, and 1000 °C with an exposure time of 3 s and step size of 0.03°. All the diffraction patterns were analyzed using a commercially available software, TOPAS®. Further, the stability of the anatase phase at a constant temperature of 700 °C was studied by heating the sample to 700 °C at the rate of 30 °C min^{-1} and holding it at the same temperature for 13 h.

The absorption spectra were recorded using a Cary 5E UV-vis-near infrared spectrometer and the photoluminescence emission spectra (at an excitation wavelength of 255 nm) were recorded in a Jobin Yvon Flurolog-3-11 spectrofluorometer.

III. RESULTS AND DISCUSSIONS

A. Structure

In the as-synthesized condition all the powders were in anatase form and no B_2O_3 could be detected through the XRD pattern when the boron content was less than 1.89%. However, in case of samples containing 1.89 wt % or more of boron, a peak corresponding to the cubic polymorph of boron oxide was observed instead of the more common hexagonal form.[37] The XRD patterns and fitted profiles of the nanocrystalline titania powder samples containing 0.5 and 1.89 wt % boron is depicted in Fig. 1. It is noteworthy that the x-ray photoelectron emission spectra taken for samples containing 1.89 and 5.5 wt % boron showed only 1*s* peaks at a binding energy value of 192.6 eV (Fig. 2). However, the chemical environment surrounding boron in B-modified TiO_2 is similar to that in pure B_2O_3, which made it difficult

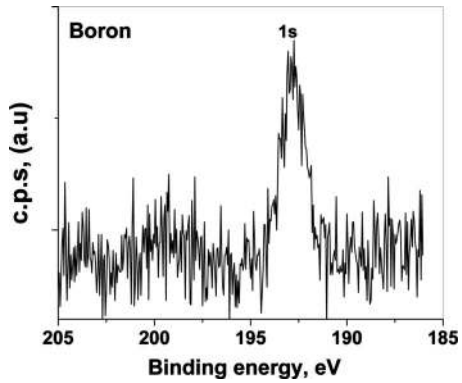

FIG. 2. XPS spectrum of B-modified TiO_2 having 1.89% boron.

TABLE I. Boron content (estimated from atomic emission spectroscopy), anatase crystallite size (estimated from XRD), and specific surface areas of synthesized powders.

Boron (wt %)	Volume averaged crystallite size (nm)	Specific surface area at room temperature ($m^2\ g^{-1}$)	Percentage reduction in surface area on annealing to 400 °C for 2h
Undoped	5	269	70%
0.5	5	287	33%
1.7	4	418	40%
3.5	4	376	26%
5.5	3	334	Nil

to unambiguously attribute the chemical environment of boron in the sample from the XPS results alone.[38] Theoretical work of Geng *et al.*[39] suggested that boron in titania, as in the case of boron oxide, can have a trigonal or tetragonal coordination. The trigonal coordination results from sp^2 hybridization whereas the tetragonal coordination results from sp^3 hybridization.

Table I lists the amount of boron as estimated by atomic emission spectroscopy, the anatase crystallite sizes estimated from the room temperature XRD patterns, and the reduction in the specific surface area (made from BET measurements) when the powders were annealed at 400 °C for 2 h. The BET measurements in all the cases showed a very high specific surface area which indicated a low degree of agglomeration in the powder particles. It was observed that on annealing at 400 °C the reduction in specific surface area of the samples were lesser in case of those containing higher boron when compared to the undoped powders. This was attributed to reduced grain growth in case of the powders with higher boron content.

High resolution transmission electron microscopy (HRTEM) images in Fig. 3 show the crystalline nature of the synthesized powders with average particle sizes of about 4 nm or less. Fourier transforms of the lattice images or the diffraction patterns did not reveal the presence of boron or any boron oxides. This was attributed to the low atomic number, well dispersed state of boron or boron oxide, and the fact that it has a lower structure factor when compared to titania.

^{11}B-magic angle spinning (MAS)-NMR spectra for samples containing 0.5, 1.89, and 5.5 wt % of boron are depicted in Fig. 4. It was seen that in the sample containing less boron, a single peak at −4.37 ppm in case of 0.5 wt % [Fig. 4(a)] and a predominant peak at −14.89 ppm in case of 1.89 wt % boron [Fig. 4(b)] were observed. On the other hand, two predominant peaks were observed at 8.6 and −3.2 ppm at a difference of about 11 ppm in case of the sample having a higher boron content of 5.5 wt % [Fig. 4(c)]. The single peak in the samples containing 0.5 and 1.89 wt % boron indicated the presence of boron predominantly in only one kind of chemical environment while, at the same time, different values of chemical shift in both the cases suggested the chemical environments in the two cases to be different. The relatively symmetrical peak at a chemical shift of −4.37

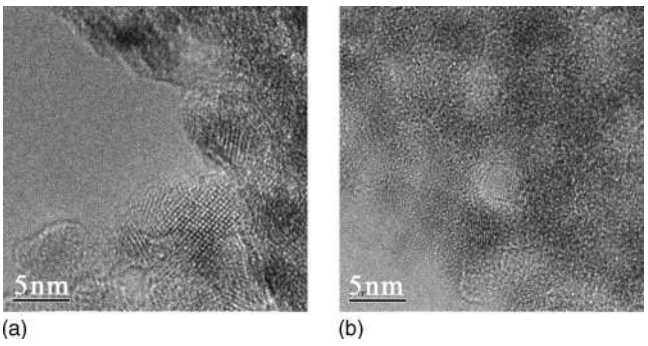

FIG. 3. HRTEM images of samples having (a) 1.7 wt % and (b) 3.6 wt % B_2O_3.

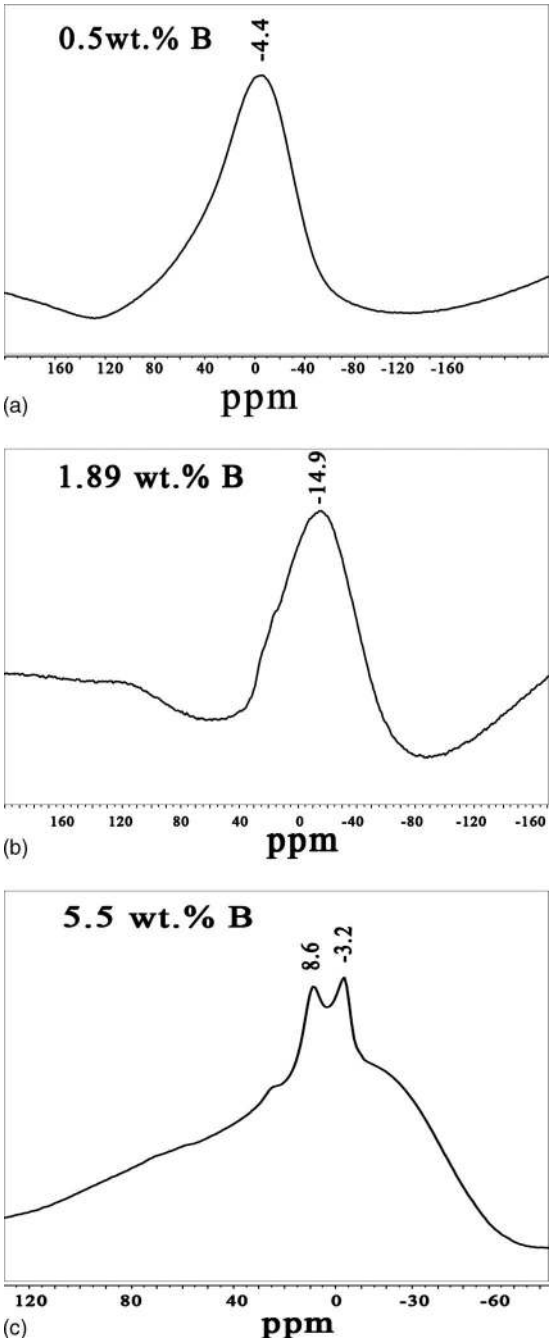

FIG. 4. ^{11}B-MAS-NMR spectra of B-modified TiO_2 containing (a) 0.5 wt %, (b) 1.89 wt % B, and (c) 5.5 wt % boron.

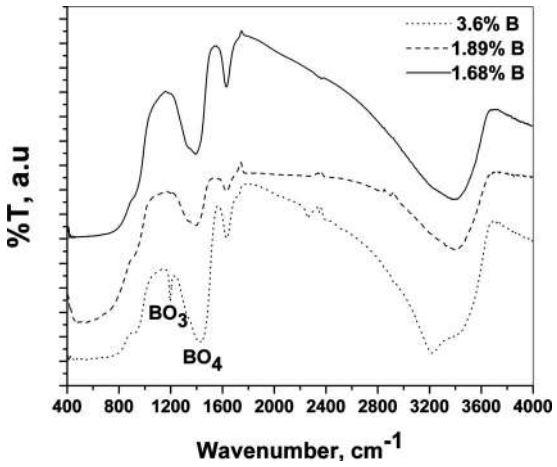

FIG. 5. FTIR spectra of B-modified TiO_2 for the different synthesized powders.

ppm in case of 0.5 wt % boron could be attributed to the chemical shift exhibiting greater shielding and a weaker quadrupole interaction of B in BO_4 structural units.[40,41] With an increase in the boron content to 1.89 wt %, the excess boron initially nucleated on the surface of titania particles/intergranular regions as BO_4 structural units prior to forming a B_2O_3 layer. Due to the different chemical environment of this surface nucleated BO_4, the peak in the NMR spectra shifted to −14.89 ppm, as reported earlier for free boron oxide.[40,42] This was also confirmed from FTIR (see later). On the other hand, for the sample containing 5.5 wt % boron two predominant peaks observed at 8.6 and −3.2 ppm at a difference of about 11 ppm indicated the presence of both BO_3 and BO_4 structural units.[42] Figure 5 depicts the FTIR spectra of the samples. In all the samples, absorption bands in the region of 3300 and 1630 cm^{-1} was attributed to stretching mode of hydroxyl group and molecular water. Absorption band in the region of 550 cm^{-1} was attributed to Ti–O–Ti stretching. Noncompensated CO_2 band could be seen in the region of 2350 cm^{-1} peaks. A broad peak at 1414 cm^{-1} indicated the presence of BO_4 structural unit in the samples containing 1.68 and 1.89 wt % boron. At the same time, for the sample having higher boron content of 3.6 wt %, a relatively sharper additional peak at 1196 cm^{-1} along with the broad peak in the region of 1414 cm^{-1} indicated the presence of both BO_3 as well BO_4 structural units.[43] Boron in lower concentration probably preferred BO_4 coordination. This was in accordance with earlier reports[43] where it was shown that the formation of B_2O_3 started with the initial nucleation of a monolayer of BO_4 structural units followed by BO_3 structural units being nucleated. In the process, until a complete monolayer was formed the specific surface area would keep increasing and once the layer had formed further formation of B_2O_3 only led to an increase in particle size and a consequent decrease in the specific surface area. This behavior is clearly seen in Fig. 6, wherein the specific surface area initially increased with boron content (till the formation of a complete layer on the titania particles) and thereafter decreased with increasing boron content.

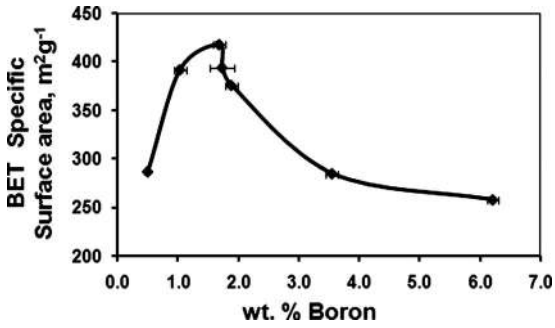

FIG. 6. Specific surface area of B-modified TiO_2 as a function of boron content.

B. High temperature anatase stability

Figure 7 depicts the high temperature XRD patterns between 300 and 1000 °C taken at intervals of 100 °C of the sample containing 3.6 wt % boron. At room temperature the samples were purely anatase. As the temperature was raised above 400 °C, the anatase (101) peak at 2θ value of 25.4° became sharper which indicated some crystallite growth. When the temperature approached 600–800 °C the rutile (110) peak (at 2θ of 27.6°) appeared. The integrated intensity of the rutile peak increased with increasing temperature while at the same time the anatase peak intensity kept reducing and finally vanished in the temperature range of 800–950 °C. The same trend was observed in case of all the boron modified nanocrystalline titania powders. However, the actual transformation temperature ranges for samples containing different amounts of boron were different. Figure 8 depicts the anatase fraction as a function of the temperature in case of all the samples synthesized. It can be seen that as the boron content in the sample increased the transformation to rutile took place at higher temperatures. For example, the sample containing 0.5 wt % boron started transforming to rutile when the temperature was about 600 °C and by the time the temperature reached 700 °C there was only about 20% anatase left untransformed. On the other hand, anatase to rutile transformation in the 6.2 wt % boron sample started only around 750 °C and was complete by about 950 °C. It is

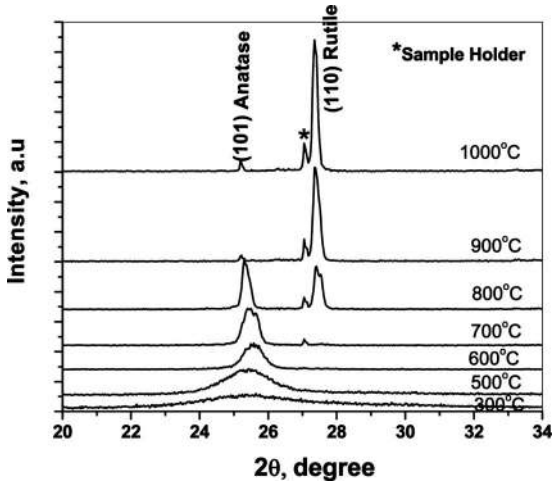

FIG. 7. XRD patterns of TiO_2 having 5.5 wt % boron at different temperatures.

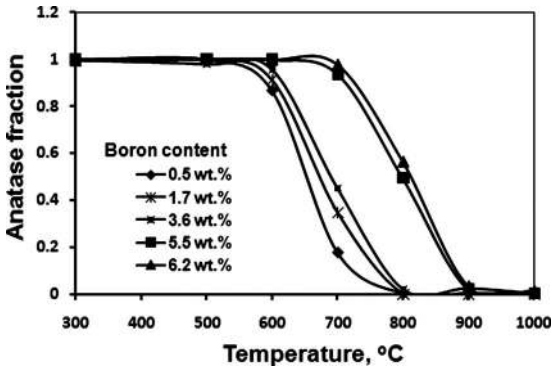

FIG. 8. Change in anatase fraction with temperature.

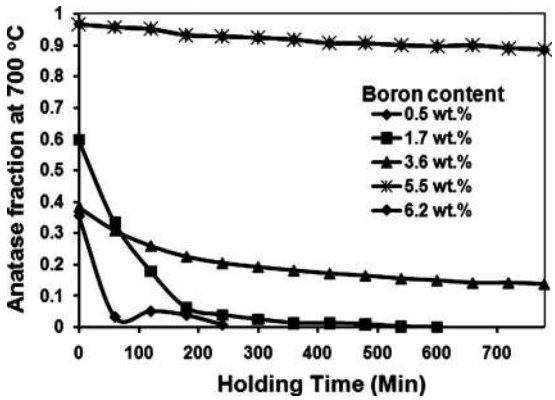

FIG. 9. Change in anatase fraction with time at 700 °C.

noteworthy that although the actual temperature at which the anatase to rutile transformation started increased with increasing boron content, the transformation temperature range in which anatase got completely converted to rutile was nearly same in all the cases. Earlier Chen *et al.*[30] reported an increase in transformation temperature of anatase to rutile which was attributed to the formation of B_2O_3 on the surface of the particles. In the present study, it was observed that the increase in temperature at which the anatase to rutile transformation started was relatively small till the boron content was about 1.7 wt %, beyond which there was a significant jump in the transformation start temperature when the boron content was 3.6 wt %. Further increase in the boron content, however, led to a minor increase in the temperature at which the transformation started. This behavior was attributed to the formation of a boron oxide layer on the surface of anatase particles/intergranular regions when heated above 500 °C due to the fact that the melting point of boron oxide is 480 °C. On further heating, B_2O_3 probably started to melt and coalesce, thereby not being effective in suppressing rutile nucleation any more and, from then on, the transformation took place at the usual rate. At boron contents of 3.6 wt % or less the boron oxide layer was not continuous over the surface of the anatase crystallites and, therefore, only some suppressions of the nucleation of rutile could take place. However, when boron content was about 5.5 wt %, it was sufficient to form a continuous boron oxide layer on the surface of the anatase crystallites which effectively suppressed the nucleation of rutile leading to a large jump in the temperature at which the transformation started.

The change in anatase fraction as a function of time for all the samples when held isothermally at 700 °C is shown in Fig. 9. It can be observed that in the samples having less than 3.6 wt % boron the rate of transformation of anatase to rutile was dependent on the boron oxide content. This was rationalized on the basis of the argument that in case of the samples with less than 3.6 wt % boron, some nucleation sites on the surface were still available due to insufficient coating of B_2O_3 on the crystallite surface, which was, in turn, a function of the amount of boron oxide present. On the other hand, the samples containing 5.5 wt % or more of boron did not show any appreciable transformation to rutile. In these samples, boron oxide had formed a continuous layer over the entire anatase particle surface/intergranular regions and was effective in hindering the nucleation of rutile. Even after holding for 13 h at 700 °C no significant anatase to rutile transformation was evident in the sample.

It is well known that in ionic crystals when the crystallite sizes are in the nanoregime, lattice expansion takes place in cubic systems whereas an expansion in *a* and a contraction in *c* takes place in noncubic tetragonal systems[44] with an overall increase in the unit cell volume. In their study, Zhao *et al.*[31] reported a contraction in the *c* parameter and possibly erroneously claimed it to be the result of boron doping while ignoring the size effect. In the present study, however, modification of nanocrystalline titania with boron led to a contraction in the lattice parameter *a* and expansion in *c* when compared to the undoped sample, as shown in Fig. 10. The *a* parameter values at room temperature were 3.767 and 3.757

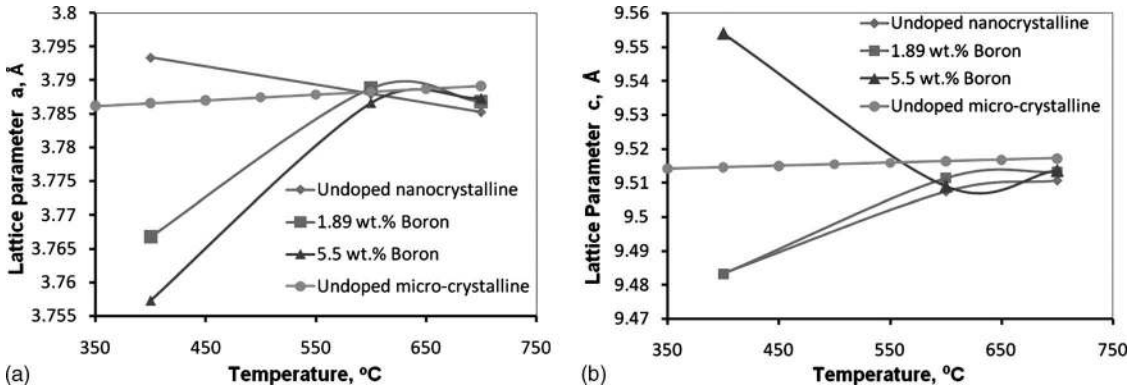

FIG. 10. Effect of boron oxide content on (a) lattice parameter *a* and (b) lattice parameter *c*, of anatase as a function of temperature.

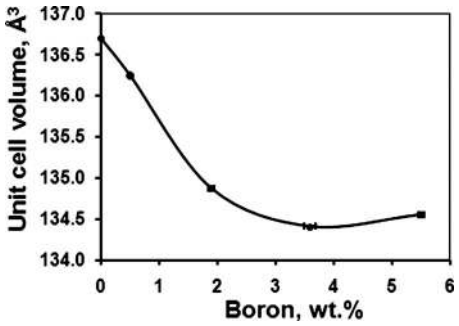

FIG. 11. Change in unit cell volume of anatase with boron content.

Å for samples containing 1.89 and 5.5 wt % boron, respectively, when compared to 3.793 Å for the undoped sample. On the other hand, a significant c parameter expansion (9.554 Å when compared to 9.514 Å for undoped sample) was observed only in case of the 5.5 wt % boron sample. This observed lattice contraction in a and expansion in c could only be the result of some amount of boron doping, unlike in the case of Zhao *et al.*[31] where the contraction in c could have arisen because of size effect. Further, it is noteworthy that an overall reduction in unit cell volume with increased boron content was observed (Fig. 11), which was in agreement with the earlier report on boron doped titania.[45] On heating to 600 °C, however, the dissolved boron was expelled from the anatase structure in the form of B_2O_3 and so the lattice parameters for pure titania and the boron modified titania became nearly the same. In earlier studies[23,26] where alumina and zirconia were used for stabilizing the anatase phase, it was argued that rutile nucleation were minimized due to the formation of solid solutions of alumina and zirconia with titania in addition to the reduction in rutile nucleation sites at the surface. In the current study, the rutile transformation took place at temperatures well over 600 °C and so the possibility of dissolved boron in the lattice affecting the transformation was ruled out.

C. Optical properties

The UV-vis spectra for the boron modified nanocrystalline titania powders are depicted in Fig. 12. A redshift in absorption edge was observed in all the boron modified samples when compared to an undoped sample. Maximum shift was observed in sample having lowest boron content of 0.5 wt %. However, the redshift was progressively lesser in samples having higher boron contents (see Fig. 12). Direct band gap was estimated from the higher absorbance region given by Ref. 46,

$$\alpha h\nu = A(h\nu - E_g)^n, \tag{1}$$

where A is a constant, $h\nu$ is the photon energy, E_g is the optical band gap, and $n=1/2$ for direct transition. E_g for direct transition in titania was estimated to be 3.71 eV for undoped nanocrystalline anatase, which was attributed to the nearly degenerate direct transition at the surface of the Brillouin zone ($X_{1a} \rightarrow X_{1b}$ and $X_{2b} \rightarrow X_{1b}$).[5,6] In the case of boron modified titania powders, the direct transition was estimated to be at 3.51, 3.60, 3.64, and 3.66 eV for the samples containing 0.5, 1.68, 1.89, and 5.5 wt % boron, respectively (as

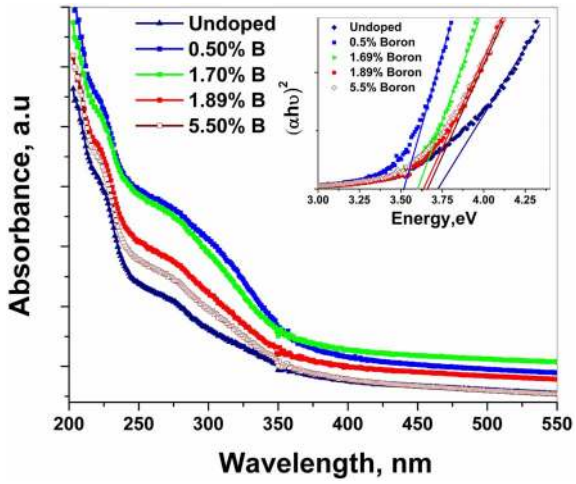

FIG. 12. (Color online) UV-vis spectra of B-modified TiO_2 with varying boron content. The inset gives the $(\alpha h\nu)^2$-energy plot.

shown in inset of Fig. 12). Earlier, Chen *et al.*[30] and Gombac *et al.*[38] observed a blueshift with boron doping which was then attributed to the reduction in crystallite size due to boron modification. On the other hand, experimental results of Zhao *et al.*[31] and Khan and Kim[45] as well as the theoretical calculations of Geng *et al.*[39] and Yang *et al.*[32] showed a redshift in the band gap due to boron doping at substitutional sites. In the current study, when the boron content in the sample was low (0.5 wt %), it entered into the structure of titania and caused a redshift resulting in a lower direct transition at 3.51 eV. However, as the boron content increased the excess boron hindered grain growth, thus resulting in lower crystallite sizes. Therefore, when the boron content was high, the redshift in the band gap due to doping was partially offset by the blueshift arising from confinement effects. This is clearly seen in Fig. 13 where the resultant redshift in the absorption edge decreased as the boron content increased.

The emission spectra of samples containing different amounts of boron are depicted in Fig. 14. The luminescence peaks in the range of 300 and 700 nm in the emission spectra were fitted with multiple Gaussian peaks using a proprietary FOCUS V1.0 program (see Fig. 15). Several luminescence peaks at wavelengths at around 280, 383, 424, 470, 545, and

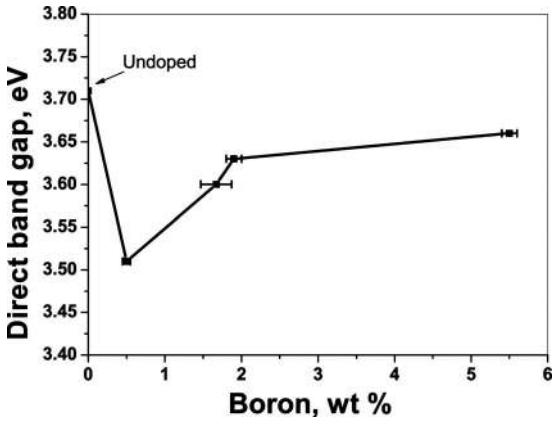

FIG. 13. Change in band gap as a function of boron content.

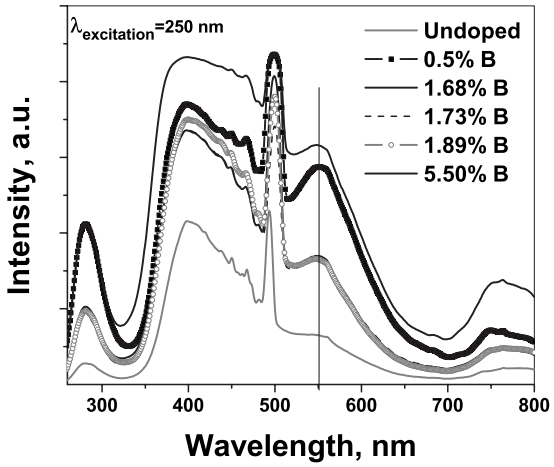

FIG. 14. Emission spectra of the as-synthesized B-modified TiO_2 at varying boron contents.

800 nm were observed. The luminescence peak at 280 nm (4.42 eV) was attributed to an allowed direct transition $\Gamma_{2'} \rightarrow \Gamma_{1b}$,[5] while the peak at 383 nm (3.23 eV) was attributed to the indirect transition $\Gamma_3 \rightarrow X_{1b}$.[5,6] Several luminescence centers just below the conduction band have been reported. Shallow traps at 0.76 and 0.8 eV below conduction band were attributed to the oxygen vacancies[5] while another trap at 0.9 eV below the conduction band was reported to be due to Ti^{4+} in the vicinity of oxygen vacancies.[5,47] In the current study the luminescence peak at 424 nm (2.92 eV) arose due to the electron transition from oxygen vacancies to the valence band while the luminescence peak observed at 545 nm was attributed to the Ti^{4+} ions in the vicinity of oxygen vacancies. The intensity of the peak at 545 nm (2.25 eV) was normalized with respect to the indirect band edge luminescence at around 383 nm and the variation of the normalized intensity with the boron content is depicted in Fig. 16. It is evident that boron modification of titania resulted in enhanced luminescence at 545 nm. The ratio I_{545}/I_{383} between the integrated intensities of peaks at 545 and 383 nm were in the range of 1.6–2.5 for the boron modified samples while it was 0.5 for the unmodified sample. This was probably because of the large number of Ti^{4+} sites in the boron modified

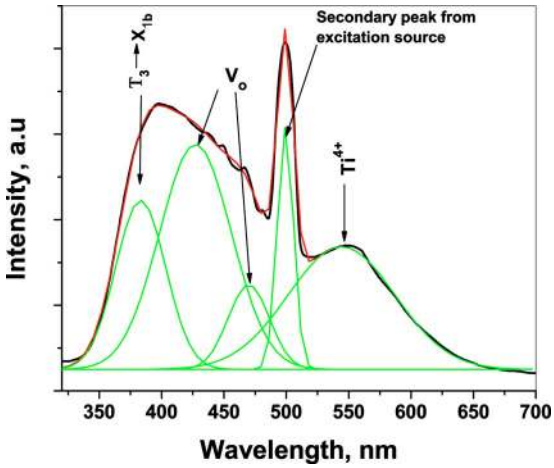

FIG. 15. (Color online) Different luminescence peaks used for fitting the emission spectrum in case of the sample containing 1.7 wt % boron.

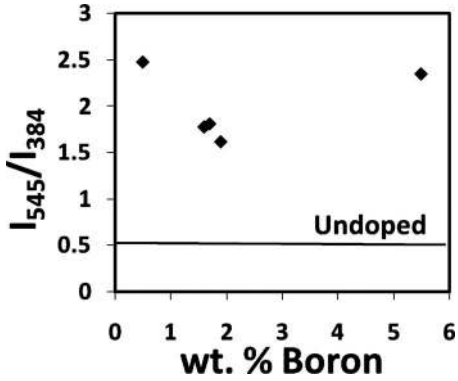

FIG. 16. Intensity variation of the luminescence peak at 545 nm (normalized with band edge luminescence) with boron content.

samples. However, the role of boron in enhancement of luminescence at 545 nm requires thorough investigation which is beyond the scope of the present study. The emission peak at 779 nm (Fig. 14) was due to the presence of Ti^{3+}.[48] The intensity of the peak at 779 nm was found to increase with increasing boron content. This was attributed to the fact that boron due to its greater affinity for oxygen when compared to titanium, resulted in more Ti^{3+} sites.

IV. CONCLUSIONS

Boron modified anatase titania nanoparticles with varying boron content were prepared in a single step by a chemical vapor synthesis process. When present in small quantities boron entered the titania structure and lowered the band gap energy. Increasing the boron content resulted in the formation of boron oxide on the surface of the anatase crystallites, which systematically raised the anatase to rutile transformation temperature. However, this resulted in progressively finer crystallite sizes and partially offset the redshift due to the confinement effects. Addition of boron to titania also enhanced the luminescence peak at 545 nm and resulted in the generation of more Ti^{3+} sites.

ACKNOWLEDGMENTS

I.A. would like to thank DAAD, Bonn, Germany for providing the financial support. I.A. would also like to pay his gratitude to Jens Suffner, Thorsten Enz, and Azad Darbandi for their help in carrying out experiments during his stay at the Gemienschaftslabor Nanomaterialien, Merialwissenschaft, Technische Universitat, Darmstadt, Germany for 6 months. S.S.B. would like to thank the Alexander von Humboldt Foundation, Bonn, Germany for providing financial support for a 1 month stay at the Darmstadt University of Technology, Darmstadt, Germany.

[1]T. Ohno, K. Sarukawa, and M. Matsumura, New J. Chem. **26**, 1167 (2002).
[2]P. V. Kamat and N. M. Dimitrijevi, Sol. Energy **44**, 83 (1990).
[3]S. A. Larson and J. L. Falconer, Appl. Catal., B **4**, 325 (1994).
[4]O. Carp, C. L. Huisman, and A. Reller, Prog. Solid State Chem. **32**, 33 (2004).
[5]N. Serpone, D. Lawless, and R. Khairutdinovt, J. Phys. Chem. **99**, 16646 (1995).
[6]N. Daude, G. Gout, and C. Jouanin, Phys. Rev. B **15**, 3229 (1977).
[7]K. Eufinger, D. Poelman, H. Poelman, R. De Gryse, and G. B. Marin, J.

Phys. D: Appl. Phys. **40**, 5232 (2007).
[8]J. Gonzalez and S. Gelover Santiago, Semicond. Sci. Technol. **22**, 709 (2007).
[9]H. Zhang and J. F. Banfield, J. Mater. Chem. **8**, 2073 (1998).
[10]A. A. Gribb and J. F. Banfield, Am. Mineral. **82**, 717 (1997).
[11]H. Zhang and J. F. Banfield, Chem. Mater. **17**, 3421 (2005).
[12]K. Porkodi and S. Daisy Arokiamary, Mater. Charact. **58**, 495 (2007).
[13]A. W. Czanderna, C. N. R. Rao, and J. M. Honig, Trans. Faraday Soc. **54**, 1069 (1958).
[14]A. Di Paola, G. Marc, L. Palmisano, M. Schiavello, K. Uosaki, S. Ikeda, and B. Ohtani, J. Phys. Chem. B **106**, 637 (2002).
[15]R. Asahi, T. Morikawa, T. Ohwaki, K. Aoki, and Y. Taga, Science **293**, 269 (2001).
[16]E. Barborini, A. M. Conti, I. Kholmanov, P. Piseri, A. Podesta, P. Milani, C. Cepek, O. Sakho, R. Macovez, and M. Sancrotti, Adv. Mater. (Weinheim, Ger.) **17**, 1842 (2005).
[17]T. Umebayashi, T. Yamaki, H. Itoh, and K. Asai, Appl. Phys. Lett. **81**, 454 (2002).
[18]W. Zhao, W. Ma, C. Chen, J. Zhao, and Z. Shuai, J. Am. Chem. Soc. **126**, 4782 (2004).
[19]J. C. Yu, J. Yu, W. Ho, Z. Jiang, and L. Zhang, Chem. Mater. **14**, 3808 (2002).
[20]K. V. Baiju, C. P. Sibu, K. Rajesh, P. Krishna Pillai, P. Mukundan, K. G. Warrier, and K. Wunderlich, Mater. Chem. Phys. **90**, 123 (2005).
[21]C. N. R. Rao, A. Turner, and J. M. Hanig, J. Phys. Chem. **11**, 173 (1959).
[22]S. Rajesh Kumar, C. Pilai, U. S. Hareesh, P. Mukundan, and K. G. K. Warrier, Mater. Lett. **43**, 286 (2000).
[23]J. Yang and J. M. F. Ferriera, Mater. Res. Bull. **33**, 389 (1998).
[24]O. Yamaguchi and Y. Mukaida, J. Am. Ceram. Soc. **72**, 330 (1989).
[25]J. Yang, Y. X. Huang, J. Maria, and F. Ferreira, J. Mater. Sci. Lett. **16**, 1933 (1997).
[26]J. Yang and J. M. F. Ferreira, Mater. Lett. **36**, 320 (1998).
[27]C. S. Enache, J. Schoonman, and R. van de Krol, Appl. Surf. Sci. **252**, 6342 (2006).
[28]Y. Sun, T. Egawa, L. Zhang, and X. Yao, Jpn. J. Appl. Phys., Part 1 **41**, L945 (2002).
[29]S. C. Pillai, P. Periyat, R. George, D. E. McCormack, M. K. Seery, H. Hayden, J. Colreavy, D. Corr, and S. J. Hinder, J. Phys. Chem. C **111**, 1605 (2007).
[30]D. Chen, D. Yang, Q. Wang, and Z. Jiang, Ind. Eng. Chem. Res. **45**, 4110 (2006).
[31]W. Zhao, W. Ma, C. Chen, J. Zhao, and Z. Shuai, J. Am. Chem. Soc. **126**, 4782 (2004).
[32]K. Yang, Y. Dai, and B. Huang, Phys. Rev. B **76**, 195201 (2007).
[33]K. A. Kranthi, S. S. Bhattacharya, M. Winterer, and H. J. Hahn, J. Phys. D: Appl. Phys. **39**, 2248 (2006).
[34]S. Seifried, M. Winterer, and H. Hahn, Chem. Vap. Deposition **6**, 239 (2000).
[35]S. Klein, M. Winterer, and H. Hahn, Chem. Vap. Deposition **4**, 143 (1998).
[36]M. Winterer, *Nanocrystalline Ceramics: Synthesis and Structure* (Springer, New York, 2002).
[37]C. T. Prewitt and R. D. Shamon, Acta Crystallogr., Sect. B: Struct. Crystallogr. Cryst. Chem. **24**, 869 (1968).
[38]V. Gombac, L. De Rogatis, A. Gasparotto, G. Vicario, T. Montini, D. Barreca, G. Balducci, P. Fornasiero, E. Tondello, and M. Graziani, Chem. Phys. **339**, 111 (2007).
[39]H. Geng, S. Yin, X. Yang, Z. Shuai, and B. Liu, J. Phys.: Condens. Matter **18**, 87 (2006).
[40]L. J. Q. Maia, V. R. Mastelaro, J. F. Schneider, P. Parent, and C. Laffon, J. Solid State Chem. **178**, 1452 (2005).
[41]L. Forni, G. Fornasari, C. Tosi, F. Trifiro, A. Vaccari, and F. Dumeignil, Appl. Catal., A **248**, 47 (2003).
[42]Y. Kim and R. J. Kirkpatrick, Geochim. Cosmochim. Acta **70**, 3231 (2006).
[43]B.-Q. Xu, S.-B. Cheng, S. Jiang, and Q. Zhu, Appl. Catal., A **188**, 361 (1999).
[44]V. Perebeinos, S.-W. Chan, and F. Zhang, Solid State Commun. **123**, 295 (2002).
[45]R. Khan and S. W. Kim, Mater. Chem. Phys. **112**, 167 (2008).
[46]J. Tauc, R. Grigorovici, and A. Vancu, Phys. Status Solidi **15**, 627 (1966).
[47]G. Redmond, D. Fitzmaurice, and M. Gratzel, J. Phys. Chem. **97**, 6951 (1993).
[48]Y. Liu and R. Claus, J. Am. Chem. Soc. **119**, 5273 (1997).

Journal of Applied Physics is copyrighted by the American Institute of Physics (AIP). Redistribution of journal material is subject to the AIP online journal license and/or AIP copyright. For more information, see http://ojps.aip.org/japo/japcr/jsp